Breakup of ^{12}C resonances into three α particles

O. S. Kirsebom,[1,*] M. Alcorta,[2] M. J. G. Borge,[2] M. Cubero,[2] C. A. Diget,[3,†] R. Dominguez-Reyes,[2] L. M. Fraile,[4,‡]
B. R. Fulton,[3] H. O. U. Fynbo,[1] S. Hyldegaard,[1] B. Jonson,[5] M. Madurga,[2,§] A. Muñoz Martin,[6] T. Nilsson,[5] G. Nyman,[5]
A. Perea,[2] K. Riisager,[1] and O. Tengblad[2]

[1]*Department of Physics and Astronomy, Aarhus University, DK-8000 Århus C, Denmark*
[2]*Instituto de Estructura de la Materia, CSIC, ES-28006 Madrid, Spain*
[3]*Department of Physics, University of York, York YO10 5DD, United Kingdom*
[4]*PH Department, CERN, CH-1211 Geneva 23, Switzerland*
[5]*Fundamental Physics, Chalmers University of Technology, SE-41296 Göteborg, Sweden*
[6]*CMAM, Universidad Autonoma de Madrid, Cantoblanco, ES-28049 Madrid, Spain*
(Received 3 May 2010; published 18 June 2010)

The reaction ^{3}He $+$ ^{11}B $\rightarrow d + {}^{12}$C* has been used to populate resonances in ^{12}C up to an excitation energy
of 15 MeV. The subsequent breakup to three α particles has been measured in complete kinematics. Dalitz plots
are used to visualize and analyze the data. The Dalitz plot intensity distribution exhibits zero points characteristic
of the total spin and parity of the 3α system allowing us to determine the spin and parity of a state in ^{12}C at
13.35 MeV whose quantum numbers were hitherto not well established. The Dalitz plot intensity distributions of
the 2^- state at 11.83 MeV and the 1^+ state at 12.71 MeV are compared with the predictions of a recent three-body
calculation as well as with simpler models. All are able to reproduce the gross structures seen in the Dalitz plot,
but none give an accurate description of the detailed profile of the distributions.

I. INTRODUCTION

In two-body decay, the decay fragments are emitted back-to-back, their energies fixed by the conservation laws of
energy and momentum. If the decaying nucleus has been prepared in a polarized state, its spin and parity can be inferred
from the angular distribution of the decay. However, if the initial spin is randomly oriented or zero, the only measurable
quantities left holding information on the structure of the initial state are the decay width and, if several decay channels are
open, the branching ratios. For three-body decay, the situation is different. The energies of the decay fragments are not
fixed but may vary within bounds determined by energy and momentum conservation thereby giving rise to measurable
energy distributions which may or may not hold additional information on the structure of the initial state. However, the
interpretation of the measured energy distributions in terms of the initial structure is complicated by final-state interactions
of both nuclear and electromagnetic origin.

The ^{12}C nucleus becomes unstable with respect to α decay at an excitation energy of 7.27 MeV. Since the daughter
nucleus, ^{8}Be, is unbound, the decay invariably leads to a final state consisting of three α particles. In the excitation
region just above the triple-α threshold, one finds states of both shell-model and α-cluster character, prime examples being the

1^+ state at 12.71 MeV and the famous 0^+ Hoyle state at
7.65 MeV, respectively. The coexistence of two such different excitation modes makes the low-level resonance structure
of ^{12}C a particularly interesting and challenging case, since theoretical models are usually tailored for the description of
either shell-model type or cluster-type excitations but seldom both. Experimentally, the study of the low-level resonance
structure of ^{12}C is complicated by the large natural width of cluster states [1]. Motivated by these considerations, we shall
attempt to address the following question: What does the energy distribution of the 3α breakup tell us about the properties
of the initial ^{12}C resonance? In particular, we wish to test the hypothesis put forward in Ref. [2] that the energy distribution
can be described entirely within an α-cluster model and hence is completely determined by the symmetries of the 3α system
and the effective forces acting between the α particles.

The fundamental quantum-mechanical phenomena of interference and tunneling are central to the description
of the 3α breakup and manifest themselves in the shape of the measured energy distributions in a nontrivial way.
A proper modeling of the breakup is needed to interpret the measurement in terms of these fascinating quantum
phenomena. Furthermore, we may test our understanding of the effective forces acting between α particles. Evidently, the
dynamics of the breakup are of great interest in their own right and not just an obstacle to be overcome in order to glimpse
into the initial structure of the decaying ^{12}C resonance.

A number of experimental studies of the 3α breakup exist in the literature, see, e.g., Refs. [3–8], most of which have
focused on the 1^+, $T = 0$ state at 12.71 MeV. To advance our understanding of the 3α breakup, we must be able to test
the theoretical models against other states at different energies and with different constraints from symmetry. We have met
this challenge by populating ^{12}C resonances through the

---

*Corresponding author: oliskir@phys.au.dk

†Present address: Department of Physics, University of York, York YO10 5DD, UK.

‡Present address: Grupo de Física Nuclear, Facultad de Ciencias Físicas, Universidad Complutense, ES-28040 Madrid, Spain.

§Present address: Physics Division, Oak Ridge National Laboratory, Oak Ridge, Tennessee 37831, USA.

064313-1

reaction ^{3}He $+ ^{11}$B $\rightarrow d + ^{12}$C* and measuring their subsequent breakup in complete kinematics.

The 3α breakup of the 12.71 MeV state was first measured in complete kinematics in 2003 by Fynbo *et al.* [8], who used the β decay of ^{12}N to populate the 12.71 MeV state. Dalitz plots were used to analyze the data. The intensity distribution was compared with the predictions of the sequential and the democratic model, see Sec. II. The gross structures were correctly reproduced by both models. When considering the detailed shape of the intensity distribution, the sequential model was found to be in much better agreement with the experimental data than the democratic model. The level of agreement was surprisingly good considering the short lifetime of the 2^+ resonance in ^{8}Be. It was pointed out that a genuine quantum-mechanical three-body calculation is needed to get a complete description of the data. Such calculations have since become available for a number of states in ^{12}C [9] and will be compared with our new measurements.

Unbound quantum-mechanical three-body systems occur in many realms of physics ranging from molecular to particle physics and attract great interest. One well-known example is the decay of mesonic resonances to three pions [10], which bears many similarities to the 3α breakup.

This paper is structured in the following way: Section II reviews the sequential and democratic breakup models. Section III briefly reviews the Dalitz plot analysis technique and discusses the origin of structures in the Dalitz plot. Section IV describes the experimental approach. Section V presents the data and makes comparisons with theoretical models. Section VI examines the challenges posed by very broad resonances. Finally, Sec. VII summarizes and concludes the study.

II. BREAKUP MODELS: LIMITING CASES

Historically, two very different breakup models (and variations thereof) have been employed to describe the experimental data. These are the sequential [7] and the democratic [11] (also called direct) models which represent limiting cases of the possible three-body decay modes.

In the sequential model, the three-body breakup is thought to proceed through an intermediate long-lived two-body resonance thereby effectively reducing the problem to that of a succession of two two-body decays, the only correlations between the two decays being those owing to conservation of angular momentum and parity. The central assumption is that of dynamical independence: At the time of the secondary breakup, the particle emitted in the primary decay must have traveled far enough for it not to feel the effects of the secondary breakup. The nuclear force quickly ceases to be important, whereas the effects of the Coulomb force are significant up to at least ~100 fm. The usefulness of the sequential model stems from the fact that we know how to deal with nuclear two-body breakups. The appropriate formalism is that of the R-matrix theory [12,13], which provides a parametrization of the nuclear resonances in terms of level energies and reduced widths and gives the penetration factors associated with the tunneling process through the Coulomb and centrifugal barriers, thus enabling us to calculate the energy distribution of the decay products. The form of the angular correlations depends on the
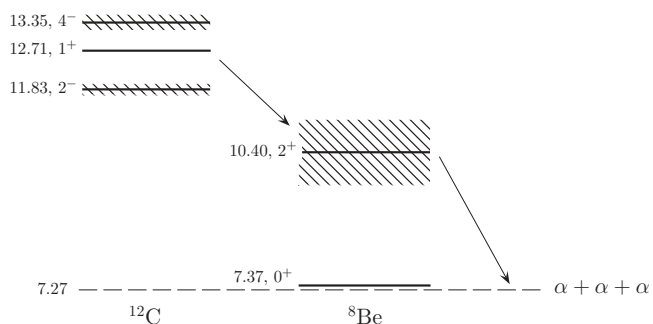

FIG. 1. Sequential decay via the broad 2^+ resonance in ^{8}Be. Energies are in MeV with respect to the ground state of ^{12}C. Only the three ^{12}C states considered in the present work are shown.

spins and orbital angular momenta involved in the decay [14]. In the case of the 3α breakup, the decay amplitude must be symmetrized in the coordinates of the three particles as required by Bose statistics causing sizable interference effects.

For the low-lying resonances in ^{12}C, two options exist. These are, as shown in Fig. 1, the narrow 0^+ ground state of ^{8}Be and its broad 2^+ first excited state. Due to the long lifetime of the ^{8}Be ground state ($\Gamma = 5.6$ eV), decays proceeding along this route may be regarded as exclusively sequential. The energies of the α particles are fixed and angular correlations absent due to the ground state having zero spin. Consequently, no dynamical information may be extracted from the ground-state channel. The ^{8}Be(2^+) channel, on the other hand, is much richer in information. For unnatural-parity states, the ground-state route is not allowed because it violates parity conservation. For natural-parity state structural information may be obtained from the branching ratios [15].

The short lifetime of the 2^+ resonance in ^{8}Be ($\Gamma = 1.5$ MeV) casts serious doubt on the validity of the sequential model. One may estimate the typical distance traveled by the first α particle at the time of the secondary breakup to be only ~5 fm, implying a Coulomb energy of ~1 MeV. This, clearly, is incompatible with the assumption of dynamical independence. Therefore, we cannot expect perfect agreement between experiment and the predictions of the sequential model. The Coulomb barrier for the secondary breakup ought to be modified from that assumed in the R-matrix formalism. One might even argue that the concept of a two-body resonance becomes meaningless due to strong perturbation caused by the near presence of the third body. In any case, great caution must be exerted in the interpretation of the experimental data [16]. The importance of final-state Coulomb repulsion may be crudely estimated by numerically solving the classical equations of motion of the 3α system subject only to the Coulomb force from a fixed distance and outward, see e.g., Refs. [17,18]. Our calculations confirm what one would naturally expect: For coaxial emission, the first α particle gets an additional "kick" so its energy increases. For emission angles close to $90°$, the Coulomb repulsion weakens because the secondary α particles move apart, and hence the first α particle gets less energy. Our calculations suggest that for coaxial emission, the extra energy imparted to the first α particle could easily be several hundred keV. The angle

measured at infinity could change as much as $10°$ compared to the actual emission angle.

Democratic decays may be regarded as the counterpart of sequential decays. Put somewhat simply, a breakup is characterized as democratic if it does not involve any long-lived intermediate states. The α-α interaction is assumed to play an insignificant role in the breakup, and the decay amplitude is calculated by expanding in hyperspherical harmonics functions (eigenstates of the grand angular momentum operator of the three-body system, characterized by the hypermomentum K) retaining only the lowest-order term permitted by symmetries. This procedure may be regarded as the three-body equivalent of a well-known procedure applied to two-body breakups: Expand the amplitude in spherical harmonics functions (angular momentum eigenstates) and neglect higher-order terms suppressed by the enhanced centrifugal barrier. Since three-body configurations of small relative two-body momenta are associated with large values of the hypermomentum K, such configurations are excluded from the democratic model. The democratic decay amplitude must be symmetrized in the coordinates of the three particles as required by Bose statistics.

III. DALITZ PLOT ANALYSIS TECHNIQUE

Assuming an unpolarized initial state, the measurement of two energies, E_1 and E_2, gives complete kinematical information. The data are best visualized in a Dalitz plot [19], see Fig. 2. Since the density of final states is proportional to $dE_1\, dE_2$, the intensity of the Dalitz plot will be proportional to the matrix element square. Consequently, pure phase-space decays result in flat distributions. Structures in the Dalitz plot may be manifestations of symmetries of the three-body system, or they may originate from final-state interactions such as a two-body resonance. Two-dimensional plots are ill suited for visual comparison of experimental and theoretical distributions at the detailed level. For this purpose, one-dimensional projections like the radial (ρ) and angular (φ) projections shown in Fig. 2 are much more useful. Other projections may be more instructive depending on the circumstances.

The role of symmetries in three-pion decays was studied by Zemach in 1964 [20]. Solely on the grounds of Bose statistics and conservation of spin, isospin, and parity, he was able to show that the decay amplitude takes on certain
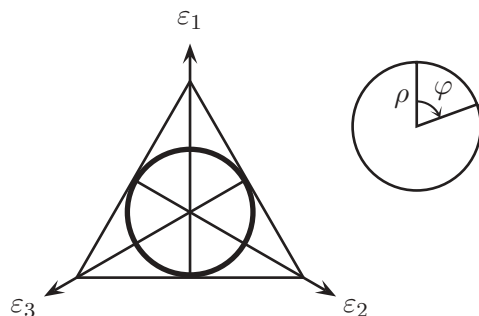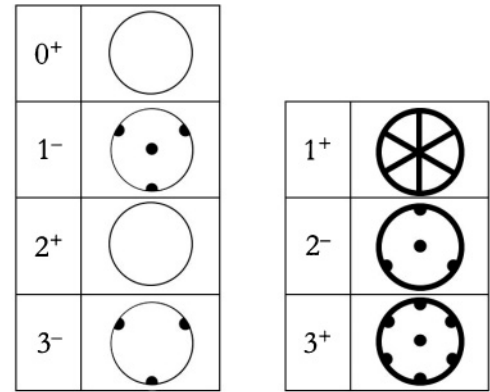

FIG. 3. Regions of the 3α Dalitz plot where the intensity must vanish (forbidden regions) are shown in black. The vanishing is of higher order where the black lines and dots overlap. The pattern for a spin $J + 2n$ ($J \geqslant 2$ and $n = 1, 2, 3, \ldots$) is identical to the pattern for spin J except that the vanishing at the center is not required for spins $\geqslant 4$.

general forms depending on the spin, isospin, and parity of the system, forcing the amplitude to vanish in specific regions of the Dalitz plot which we shall refer to as *forbidden* regions. Zemach made no assumptions about the interactions involved except that they have to conserve isospin and parity. Pions and α particles are both spin-zero bosons but have opposite parities (negative and positive, respectively) and, in contrast to α particles, pions possess a nonzero isospin of $T = 1$. The results of Zemach's analysis can readily be applied to the 3α system as long as we account for the difference in parity and restrict ourselves to 3π systems of total isospin $T = 3$. The regions of the 3α Dalitz plot forbidden by symmetry are shown in Fig. 3. Generally, the restrictions imposed by the symmetries of the 3α system are more severe for the unnatural-parity states. While severe constraints may facilitate spin-parity assignments, mild constraints make it easier to study the effects of interactions.

In a sequential decay of ^{12}C through a two-body resonance, the first α particle gets two-thirds of the energy released in the primary decay. The center of mass energies of the two secondary α particles depend on the orientation of the secondary breakup relative to the first. Consequently, the intensity of the Dalitz plot will be confined to bands like those shown in Fig. 4, whose width and distance to the sides of the triangle reflect the width and energy of the
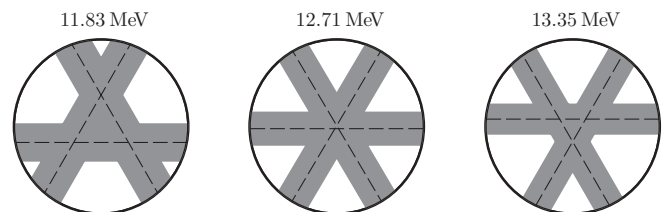

FIG. 2. Dalitz plot and associated projections, ρ and φ. ε_i denotes the energy of the ith α particle normalized to the total decay energy, i.e. $\varepsilon_i = E_i / \sum_k E_k$.

FIG. 4. Sequential band structure associated with the decay of the three ^{12}C states considered in the present work. The dotted lines indicate the maximum of the band's lateral intensity distribution; the gray area its width (FWHM).

two-body resonance. The lateral intensity distribution of the bands depends on the profile of the two-body resonance as well as the penetration factors associated with the Coulomb and centrifugal barriers of the entrance ($\alpha + {}^8$Be) and exit ($\alpha + \alpha$) channels, while the longitudinal structure is determined by the angular correlations. Where bands overlap, interference effects may be expected.

Figures 3 and 4 are useful points of reference when inspecting the two-dimensional Dalitz distributions measured in experiment or calculated from theory. Conceptually, the separation of structures in two distinct groups, namely, those due to the general symmetries of the 3α system and those caused by final-state interactions, is very useful: Any theoretical model possessing the correct symmetries is bound to reproduce the *gross* structures of the Dalitz distribution irrespective of its assumptions about the dynamics of the 3α system. The forbidden regions identified in Fig. 3 also have a more "practical" application. As we shall see, they serve as a model-independent spectroscopic tool which allows us to determine or at least impose constraints on the spin-parity of ^{12}C resonances. See Ref. [21] for an example of such an application in particle physics. Notice that the mere existence of a zero point in the Dalitz plot (i.e., a region of vanishing intensity) cannot be used as conclusive evidence for a particular spin-parity assignment because there could also be dynamical reasons for the suppressed intensity. However, the absence of a zero point can always be used to falsify a proposed spin-parity assignment.

IV. EXPERIMENTAL APPROACH

In the present study, ^{12}C resonances were populated through the reaction ^{3}He $+ ^{11}$B $\rightarrow d + ^{12}$C* and their subsequent breakup was measured in complete kinematics. The experiment was performed at the Centro de Microanálisis de Materiales in Madrid [22] at a beam energy of 8.5 MeV. The detection system consisted of four double-sided silicon strip detectors (DSSSD) 60 μm thick [23], each backed by an unsegmented silicon detector 1.5 mm thick allowing for particle identification. The intrinsic resolution (full width at half maximum, FWHM) of the DSSSDs was 35 keV, while the resolution of the backing detectors was 40–50 keV. The detectors were placed as shown on Fig. 5, 4 cm from the target with two of them covering $7°$–$75°$ to the beam and two others covering $98°$–$170°$, thereby obtaining a total solid-angle coverage of 38% of 4π. One DSSSD has 32×32 strips of 2 mm width, the other three 16×16 strips of 3 mm width, resulting in an angular resolution of $2°$ and $3°$, respectively. A detailed description of the experimental apparatus and methods is given in Ref. [24], which also explains the initial steps of the analysis concerned with the transformation of raw data into physics events.

The complete kinematical information allows us to separate decays according to whether they proceed via the ground state of ^{8}Be or not as shown in Fig. 6. The ^{12}C excitation energy is calculated from the energy and the angle of the deuteron. Five states are readily visible: the 3^- state at 9.64 MeV, the 1^- state at 10.84 MeV, the 2^- state at 11.83 MeV, the 1^+ state at 12.71 MeV, and finally a state at 13.35 MeV whose spin and
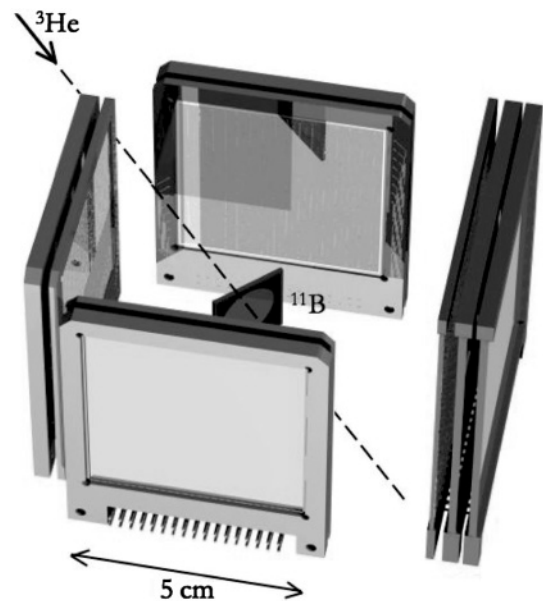

FIG. 5. Complete kinematics detection setup consisting of four DSSSDs 60 μm thick, each backed by an unsegmented silicon detector 1.5 mm thick allowing for particle identification. One DSSSD has 32×32 strips of 2 mm width, the other three 16×16 strips of 3 mm width, resulting in an angular resolution of $2°$ and $3°$, respectively.

parity were not well established prior to this work. In the most recent compilation [25], it is tentatively assigned spin-parity 2^-, but theoretical considerations[1] and recent experimental findings [26] seem to favor a 4^- assignment. As we will later show, the present work firmly establishes 4^- as the correct spin-parity assignment. As expected, the unnatural-parity states do not decay via the ground state of ^{8}Be, whereas the decay of the two natural-parity states predominantly follows this route. The high-energy cutoff setting in at 14.5 MeV is due to the deuterons being stopped in the DSSSD preventing particle identification through the ΔE-E method.

The spectrum in Fig. 6 is essentially free of background [24]. The intensity present in addition to the five visible peaks does not constitute background in the usual sense of the term

---

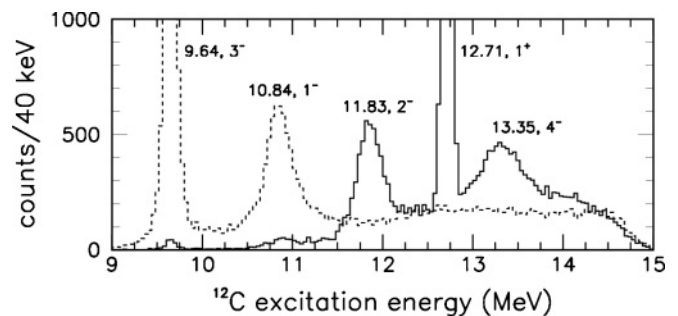[1]Cf. footnote to Table 12.6 of Ref. [25].

FIG. 6. ^{12}C excitation spectrum separated into decays that proceed via the ground state of ^{8}Be (dashed) and decays that do not (solid).
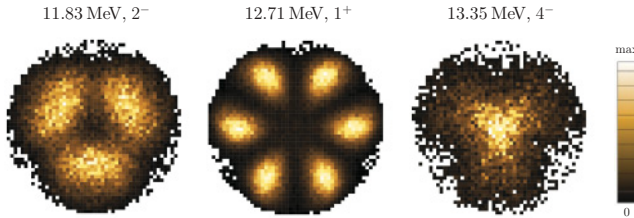
FIG. 7. (Color online) Dalitz plots obtained using the experimental data. The spin and parity of the 13.35 MeV state is given as 4^- as established by the present work, contradicting the tentative 2^- assignment that appears in the most recent $A = 12$ compilation [25].

but is understood as broad overlapping resonances in ^{12}C, possibly with small contributions from the two very broad 1^+ and 2^+ $T = 0$ states in ^{6}Li through the ^{3}He $+ ^{11}$B $\to$ ^{8}Be $+ ^6$Li $\to d + 3\alpha$ channel (reactions via the narrow 3^+, $T = 0$ state in ^{6}Li were easily removed by gating on the corresponding peak in the $d + \alpha$ relative energy spectrum). Nonetheless, we shall refer to these broad structures as "background" when we discuss their contribution to the Dalitz plots displayed in Fig. 7. A study of the actual nature of these broad structures will be published elsewhere [15]. Here we adopt the heuristic approach of using the regions adjacent to the peaks to determine the characteristics of the background below the peak. The background fractions are 11%, 8%, and 50% for the 11.83, 12.71, and 13.35 MeV states, respectively. These numbers were obtained by fitting the peaks with Breit-Wigner profiles folded through the experimental resolution in the form of a Gaussian and superimposed on a quadratic polynomial describing the shape of the background in the vicinity of the peak.

V. RESULTS

Shown in Fig. 7 are the experimental Dalitz distributions obtained by gating on the three unnatural-parity states in Fig. 6. Both multiplicity four and multiplicity three (one α goes undetected) events have been used, giving 3.5×10^4 events for the 11.83 MeV state, 1.2×10^5 events for the 12.71 MeV state, and 9.9×10^3 events for the 13.35 MeV state.

A. Spin-parity assignment

The Dalitz distributions of the 11.83 and 12.71 MeV states clearly exhibit the forbidden regions dictated by symmetry, cf. Fig. 3. What can we say about the spin and parity of the 13.35 MeV state? Since it is not observed to decay via the ground state of ^{8}Be, it is likely to have unnatural parity. The absence of a zero point at the center of the Dalitz plot excludes the spin-parity assignments 1^+, 2^-, and 3^+. As noted in the caption of Fig. 3, the pattern for a spin $J + 2n$ ($J \geqslant 2$ and $n = 1, 2, 3, \ldots$) is identical to the pattern for spin J except that the vanishing at the center is not required for spins $\geqslant 4$. Therefore, we conclude that the correct spin-parity assignment for the 13.35 MeV state is 4^- (though spins $\geqslant 5$ cannot be excluded based on the present study alone). The radial projection of the Dalitz distribution is shown in Fig. 8, demonstrating with all clarity that the intensity at the center
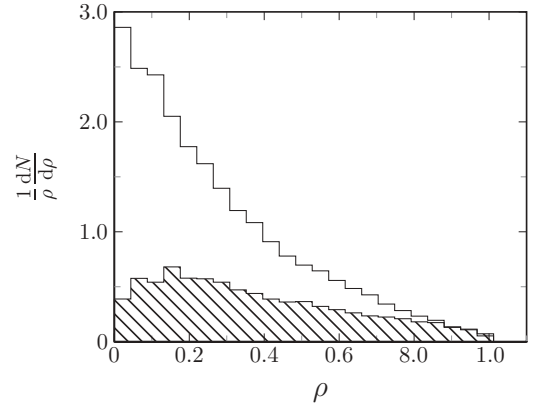

FIG. 8. Radial projection of the Dalitz plot for the 13.35 MeV state normalized to unit area. The radial coordinate ρ runs from 0 (center) to 1 (circumference). The hatched histogram represents the contribution of the background.

of the Dalitz plot is not due to background, the contribution of which is indicated by the hatched histogram. The radial projection also confirms the vanishing of the intensity at the circumference as expected for all unnatural-parity states.

B. Model comparison

The Dalitz distributions of the 11.83 and 12.71 MeV states will now be compared with the predictions of four models: The sequential and democratic models outlined in Sec. II, a slightly modified version of the sequential model conceived by Fynbo *et al.* [8], and the full three-body calculation of Ref. [9]. The predictions of the four models are shown in Figs. 9 and 10. Their radial and angular projections are compared with the experimental data in Figs. 11 and 12. "Sequential I" refers to the standard formulation of the sequential model [7] and "Sequential II" to the slightly modified version of Ref. [8].
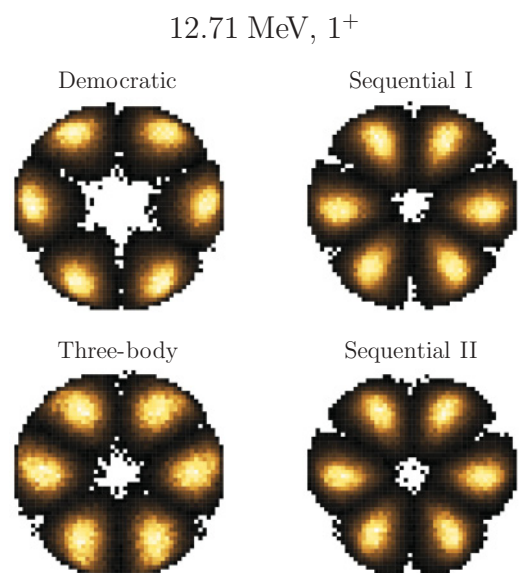

FIG. 9. (Color online) Simulations of the Dalitz distribution for the 12.71 MeV state based on four different theoretical models.
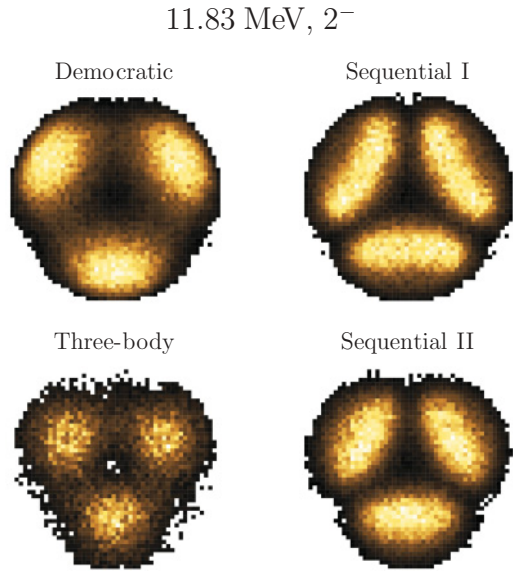
11.83 MeV, 2^-

Democratic   Sequential I

Three-body   Sequential II

FIG. 10. (Color online) Same as Fig. 9, but for the 11.83 MeV state.

a. Sequential I. In the sequential model, we use the *R*-matrix parameters of Ref. [27] for the broad 2^+ resonance in ^{8}Be: an excitation energy of $E_0 = 3037 \pm 5$ keV and a reduced width of $\gamma^2 = 1075 \pm 7$ keV. The channel radii were computed as $a = 1.42$ fm $(A_1^{1/3} + A_2^{1/3})$. The orbital angular momentum in the secondary breakup is always $l' = 2$. In the primary breakup, l depends on the spin of ^{12}C. In the case of the 12.71 MeV state, only $l = 2$ is compatible with conservation of spin and parity, whereas $l = 1, 3$ are possible for the 11.83 MeV state.

b. Sequential II. The modification introduced in Ref. [8] consists in adding extra barrier penetrabilities for each of the secondary α particles as an approximate treatment of final-state Coulomb repulsion. Further details are given in Ref. [8].

c. Democratic. The democratic model was briefly reviewed in Sec. II. For further details, see Ref. [11].

d. Three-body. The full three-body calculation of Ref. [9] treats ^{12}C as a 3α-cluster system at all distances. The three-body problem is solved in coordinate space using the adiabatic hyperspherical expansion method. The complex scaling method is used to compute resonances. The phenomenological Ali-Bodmer two-body interaction (tuned to reproduce the low-energy two-body scattering phase shifts) is used. In addition, a three-body short-range interaction adjusted to reproduce the correct excitation energies in ^{12}C is included.

To compare model calculations against the data, we must account for experimental effects. For this purpose, Monte Carlo simulations have been employed [24]. The following procedure was adopted: First, a large sample of 3α events is generated. Each event is associated with a weight factor which is simply the decay amplitude predicted by the model. These weight factors serve for the acceptance-rejection sampling performed in the Monte Carlo simulation of the ^{3}He $+ ^{11}$B $\rightarrow d + ^{12}$C$^* \rightarrow d + 3\alpha$ reaction. The angular distribution assumed for the deuteron is the one extracted
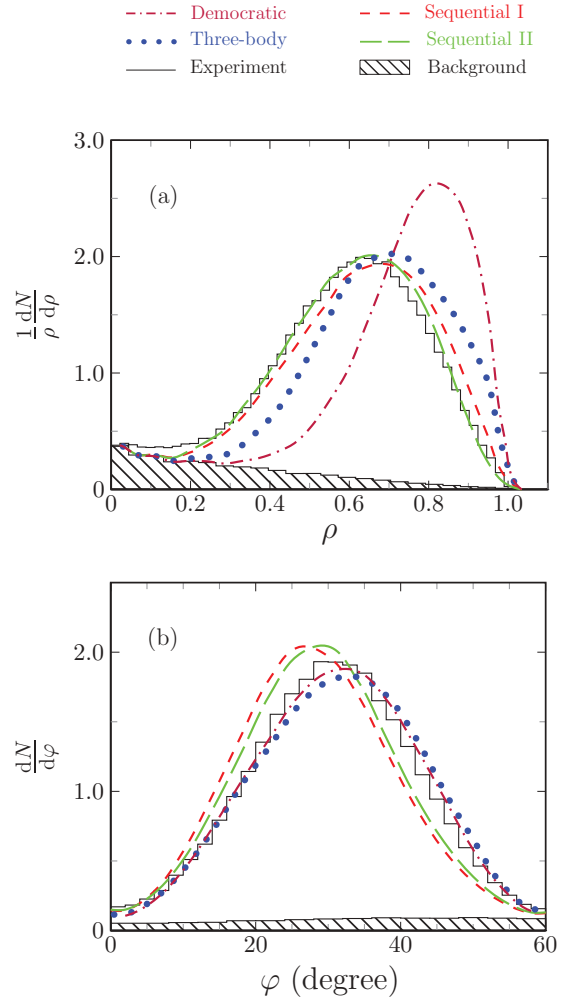

FIG. 11. (Color online) Radial and angular projections of the Dalitz plot for the 12.71 MeV state. Owing to the six-fold symmetry of the Dalitz plot, the angular projection only runs from $0°$ to $60°$.

from the experimental data which is peaked at forward angles displaying a dominant direct contribution (one-proton transfer) [15]. We take into account the geometry of the detection system and simulate the response of the individual detectors to charged-particle radiation. Finally, we pass the output of the simulation through exactly the same analysis routines as applied to the physical data hence accounting for any bias introduced by the various cuts and gates imposed on the data. The final simulated distributions contain $\sim 1.5 \times 10^5$ events. Varying the geometry, the detector resolution, and the deuteron angular distribution assumed in the simulation within their respective uncertainties, we find no visible effect on the final distributions.

The ^{12}C resonance formed in the ^{3}He $+ ^{11}$B $\rightarrow d + ^{12}$C* reaction is likely to be polarized to a lesser or larger extent, which may affect the Dalitz distributions since the experiment does not cover full 4π (such polarization has been observed in the case of the 9.64 MeV state for deuterons emitted at forward angles where the direct reaction mechanism dominates. At backward angles, the polarization disappears). The form of the polarization is not easily extracted from the measurements.
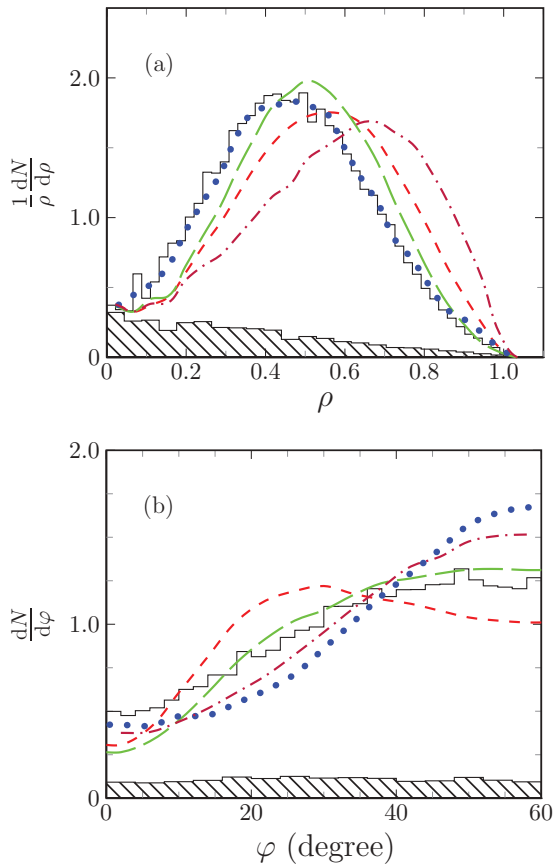
FIG. 12. (Color online) Same as Fig. 11, but for the 11.83 MeV state.

However, through simulations (based on the sequential model), we find that the Dalitz distributions of the 11.83 and 12.71 MeV states are insensitive to polarization, which may be explained as follows: Owing to the small angular momenta involved, only spherical harmonics of low order contribute, cf. Eq. (2) of Ref. [8], whose variation on the angular scale of the detectors is relatively small. For the 4^- state, the effects of polarization are no longer negligible, which is the reason why we chose to focus on the 11.83 and 12.71 MeV states for the model comparisons.

We note that the statistical uncertainties on the experimental and simulated distributions shown in Figs. 11 and 12 are essentially zero.

1. The 12.71 MeV state

All models reproduce the forbidden regions dictated by symmetry. However, they all fail in reproducing the detailed shape of the distribution as revealed by the radial and angular projections. The inclusion of final-state Coulomb repulsion in the sequential model is seen to shift the radial projection toward smaller values of ρ consistent with suppression of coaxial emission[2] whereby perfect agreement with the data

---

[2]The circumference of the Dalitz plot corresponds to the situation where all three momenta lie along the same axis.

is achieved. The angular projection is shifted toward larger values of φ, but the agreement with the data is still rather poor. The deviation is far too large to be accounted for by the uncertainties on the R-matrix parameters.

The three-body model and the democratic model in particular give poor fits to the radial projection. On the other hand, they predict angular projections in reasonable agreement with the data even though both are too wide and slightly displaced. As is evident from the sequential band structure of the 12.71 MeV state, cf. Fig. 4, the centroid and width of the angular projection directly reflect the energy and width of the two-body resonance, whereas the radial projection is, to a first approximation, independent of these parameters. If we were able to modify the α-α potential used in the three-body calculation so as to increase the energy and simultaneously reduce the width of the two-body resonance, near perfect agreement with the data could probably be achieved for the angular projection. The shifts needed are on the order of 100 keV, which is not unrealistic [28]. However, this would not improve the situation in the radial projection.

2. The 11.83 MeV state

It was noted in Ref. [11] that the democratic model ought to work better the lower the energy. However, when compared with the data, the democratic model is seen to give bad fits also for the 11.83 MeV state. The three-body model is in perfect agreement with the data in the radial projection, but it gives a poor fit in the angular projection.

An additional complication arises in the sequential model, because the $\alpha + {}^8$Be breakup may proceed both through a p wave and an f wave (in contrast, the decay of the 12.71 MeV state proceeds exclusively through a d wave). The two amplitudes must be added coherently, i.e. $f = \alpha f_{l=1} \pm \beta f_{l=3}$ with $\alpha^2 + \beta^2 = 1$ and $\alpha, \beta \geqslant 0$. The two amplitudes may interfere constructively $(+)$ or destructively $(-)$. The best fit to the data is achieved by assuming roughly equal weights, $\alpha \approx \beta \approx 1/\sqrt{2}$, and destructive interference. Note that the f-wave amplitude $f_{l=3}$ is suppressed by a factor of ≈ 5 relative to the the p-wave amplitude $f_{l=1}$ due to the increased centrifugal barrier.

The inclusion of final-state Coulomb repulsion in the sequential model is, again, seen to shift the radial distribution toward smaller values of ρ thereby improving the agreement with the data. The fit to the angular projection is also improved though deviations remain.

VI. EXTENSION TO BROAD RESONANCES

It is the presence of very broad states with a strong coupling to the 3α continuum that makes the study of the ^{12}C excitation spectrum interesting as well as challenging. Nevertheless, the present discussion has focused exclusively on three relatively narrow states, while the broad underlying (and as of yet unresolved) structures have been treated merely as a background. The obvious and challenging next step will consist in applying the Dalitz plot analysis technique to the regions *in between* the peaks in Fig. 6. In particular, it may be possible to determine or at least constrain the spin and parity of

the broad states by examining the gross structures of the Dalitz plot. However, as we consider ^{12}C states of increasing width (and hence shorter lifetime), we will eventually be confronted with a four-body problem in which dynamical correlations between the deuteron and the three α particles must be taken into account.

One indicator of the necessity of a four-body treatment is the Coulomb energy stored in the $d + {}^{12}$C system at the time of the 3α breakup. The distance separating the deuteron and the ^{12}C nucleus at the time of the 3α breakup may be estimated as $v\tau$, where $\tau = \hbar / \Gamma$ is the lifetime of the excited state in ^{12}C and v is the relative speed of the deuteron and the ^{12}C nucleus at infinite separation. If we require the Coulomb energy to be less than 10% of the energy released in the 3α breakup, we arrive at an upper limit of $\Gamma < 0.6$–1 MeV (for ^{12}C excitation energies in the range 10–14 MeV). Another indicator of the necessity of a four-body treatment is the de Broglie wavelength $\lambda = h/p$ at infinite separation. If we picture the deuteron and the ^{12}C nucleus as freely propagating wave packets, λ gives a measure of their spatial extension. In this naïve picture, a four-body description becomes necessary when λ is comparable to the distance separating the deuteron and the ^{12}C nucleus at the time of the 3α breakup. This happens when Γ exceeds 1–2 MeV.

Even though these estimates are very crude, they demonstrate that dynamical four-body correlations may become important when $\Gamma \gtrsim 1$ MeV. To avoid four-body correlations all together, alternative ways of populating excited states in ^{12}C must be found, e.g., through the β decay of ^{12}B and ^{12}N [29] or γ decays from higher-lying states in ^{12}C [30].

VII. CONCLUSION

The breakup of ^{12}C resonances into three α particles constitutes an interesting and challenging physics case from the point of view of both theory and experiment. The fundamental quantum processes of interference and barrier tunneling play a central role in the breakup, so does the α-α potential, its influence made most evident by the observation of sequential decays proceeding via the narrow ground state of ^{8}Be. They all leave their imprint on the energy distribution of the α particles. The extent to which the structure of the initial ^{12}C state affects the energy distribution is unknown.

The experimental data are best visualized in two-dimensional Dalitz plots which, in the absence of polarization, contain the complete kinematical information. The unique symmetries of the 3α system play a central role in the description of the breakup because they cause the intensity to vanish in certain regions of the Dalitz plot, thereby inducing structures that do not depend on the decay mechanism but are characteristic of the total spin and parity of the system and hence providing a model-independent spectroscopic tool that allows us to determine or at least constrain the spin and parity of the system.

In the present work, the reaction ^{3}He + ^{11}B $\rightarrow$ $d + {}^{12}$C* has been used to populate resonances in ^{12}C up to an excitation energy of 15 MeV, and the subsequent breakup into three α particles has been measured in complete kinematics. Dalitz plots for the three unnatural-parity states at 11.83,

12.71, and 13.35 MeV, which are prevented from decaying sequentially through the narrow ground state of ^{8}Be due to spin-parity conservation, were presented and analyzed. The gross structures of the Dalitz plot, in particular the absence of a zero point at the center, allowed us to assign spin-parity 4^{-} to the 13.35 MeV state in disagreement with the tentative 2^{-} assignment of the most recent $A = 12$ compilation [25] but in agreement with recent experimental findings [26] and favored by theoretical considerations.

The Dalitz distributions of the 11.83 and 12.71 MeV states were compared with the predictions of four theoretical models. All were found to reproduce the gross structures dictated by the symmetries of the system, but none were able to reproduce the detailed shape of the distributions. The sequential model modified to accommodate final-state Coulomb repulsion (Sequential II) gives the best fit to the data. As previously pointed out by [8], the sequential model in its standard form (Sequential I) gives a surprisingly good fit for the 12.71 MeV state considering the very short lifetime of the ^{8}Be(2^{+}) resonance. However, for the 11.83 MeV state, we do not find the same high level of agreement. We may understand this as a result of the relaxed constraints from symmetry leaving more room for the dynamics of the breakup process to affect the final energy distribution of the α particles.

We hinted at one possible explanation for why the full three-body computation of Ref. [9] is unable to give an accurate description of the data, namely, the α-α two-body potential which has been tuned to reproduce the measured $\alpha + \alpha$ scattering phase shifts. Following this procedure, the excitation energy of the ^{8}Be(2^{+}) state is computed to be 2.8 MeV, whereas the experimental value is 3.0 MeV [28]. However, we also argued that the discrepancies cannot be explained by this effect alone. This raises the intriguing possibility that we might be seeing the effect of the small-distance 12-nucleon structure on the energy distribution of the α particles at large distances.

Full three-body computations have also been performed for other states in ^{12}C such as the 13.35 MeV state discussed in the present paper and the 4^{+} state at 14.08 MeV. The latter may prove a particularly interesting case due to the absence of constraints from symmetry leaving plenty of room for the dynamics of the breakup to affect the energy distribution of the α particles and hence providing a most challenging case to theory. However, considering the discrepancies observed for the 11.83 and 12.71 MeV states, the need for an improved theoretical model which connects the three-body breakup to an *ab initio* 12-nucleon description of the resonance structure at small distances is already obvious.

[1] S. Hyldegaard *et al.*, Phys. Rev. C **81**, 024303 (2010).
[2] R. Álvarez-Rodríguez, A. S. Jensen, D. V. Fedorov, H. O. U. Fynbo, and E. Garrido, Phys. Rev. Lett. **99**, 072503 (2007).
[3] W. C. Olsen, W. K. Dawson, G. C. Neilson, and J. T. Sample, Nucl. Phys. **61**, 625 (1965).
[4] J. D. Bronson, W. D. Simpson, W. R. Jackson, and G. C. Phillips, Nucl. Phys. **68**, 241 (1965).
[5] M. A. Waggoner, J. E. Etter, H. D. Holmgren, and C. Moazed, Nucl. Phys. **88**, 81 (1966).
[6] W. von Witsch, M. Ivanovich, D. Rendic, V. Valkovic, and G. C. Phillips, Nucl. Phys. A **180**, 402 (1972).
[7] D. P. Balamuth, R. W. Zurmühle, and S. L. Tabor, Phys. Rev. C **10**, 975 (1974).
[8] H. O. U. Fynbo *et al.*, Phys. Rev. Lett. **91**, 082502 (2003).
[9] R. Álvarez-Rodríguez, A. S. Jensen, E. Garrido, D. V. Fedorov, and H. O. U. Fynbo, Phys. Rev. C **77**, 064305 (2008).
[10] C. Amsler, Rev. Mod. Phys. **70**, 1293 (1998).
[11] A. A. Korsheninnikov, Yad. Fiz. **52**, 1304 (1990) [Sov. J. Nucl. Phys. **52**, 827 (1990)].
[12] A. M. Lane and R. G. Thomas, Rev. Mod. Phys. **30**, 257 (1958).
[13] P. Descouvemont and D. Baye, Rep. Prog. Phys. **73**, 036301 (2010).
[14] L. C. Biedenharn and M. E. Rose, Rev. Mod. Phys. **25**, 729 (1953).
[15] M. Alcorta *et al.* (unpublished).
[16] H. O. U. Fynbo, R. Alvarez-Rodriguez, A. S. Jensen, O. S. Kirsebom, D. V. Fedorov, and E. Garrido, Phys. Rev. C **79**, 054009 (2009).
[17] E. Norbeck and F. D. Ingram, Phys. Rev. Lett. **20**, 1178 (1968).
[18] D. T. Thompson, G. E. Tripard, and D. H. Ehlers, Phys. Rev. C **5**, 1174 (1972).
[19] H. R. Dalitz, Philos. Mag. **44**, 1068 (1953).
[20] C. Zemach, Phys. Rev. **133**, B1201 (1964).
[21] M. Gaspero, B. Meadows, K. Mishra, and A. Soffer, Phys. Rev. D **78**, 014015 (2008).
[22] [http://www.cmam.uam.es/].
[23] O. Tengblad *et al.*, Nucl. Instrum. Methods A **525**, 458 (2004).
[24] M. Alcorta *et al.*, Nucl. Instrum. Methods A **605**, 318 (2009).
[25] F. Ajzenberg-Selove, Nucl. Phys. A **506**, 1 (1990).
[26] M. Freer *et al.*, Phys. Rev. C **76**, 034320 (2007).
[27] M. Bhattacharya, E. G. Adelberger, and H. E. Swanson, Phys. Rev. C **73**, 055802 (2006).
[28] R. Álvarez-Rodríguez (private communication).
[29] C. Aa. Diget *et al.*, Nucl. Phys. A **760**, 3 (2005).
[30] O. S. Kirsebom *et al.*, Phys. Lett. B **680**, 44 (2009).